



**HAL**  
open science

## Evidence of a green luminescence band related to surface flaws in high purity silica glass

Jessica Fournier, Jérôme Neauport, Pierre Grua, Evelyne Fargin, Veronique Jubera, David Talaga, Stéphane Jouannigot

### ► To cite this version:

Jessica Fournier, Jérôme Neauport, Pierre Grua, Evelyne Fargin, Veronique Jubera, et al.. Evidence of a green luminescence band related to surface flaws in high purity silica glass. *Optics Express*, 2010, 18 (21), pp.21557-21566. 10.1364/OE.18.021557 . cea-01217071

**HAL Id: cea-01217071**

**<https://cea.hal.science/cea-01217071>**

Submitted on 18 Oct 2015

**HAL** is a multi-disciplinary open access archive for the deposit and dissemination of scientific research documents, whether they are published or not. The documents may come from teaching and research institutions in France or abroad, or from public or private research centers.

L'archive ouverte pluridisciplinaire **HAL**, est destinée au dépôt et à la diffusion de documents scientifiques de niveau recherche, publiés ou non, émanant des établissements d'enseignement et de recherche français ou étrangers, des laboratoires publics ou privés.



Distributed under a Creative Commons Attribution - NonCommercial - NoDerivatives 4.0 International License

# Evidence of a green luminescence band related to surface flaws in high purity silica glass

J. Fournier,<sup>1,2\*</sup> J. Néauport,<sup>1</sup> P. Grua,<sup>1</sup> E. Fargin,<sup>2</sup> V. Jubera,<sup>2</sup> D. Talaga,<sup>3</sup> and S. Jouannigot<sup>4</sup>

<sup>1</sup> Commissariat à l'énergie atomique, Centre d'études scientifiques et techniques d'Aquitaine, BP2, F-33114, Le Barp, France

<sup>2</sup> CNRS, Université de Bordeaux, ICMCB, 87 Avenue du Dr Schweitzer, Pessac, F-33608, France

<sup>3</sup> CNRS, Université de Bordeaux, ISM, 351 cours de la libération, Talence F-33405, France

<sup>4</sup> Laboratoire des Composites Thermo-Structuraux, LCTS-UMR 5801 (CNRS-SAFRAN-CEA-University of Bordeaux 1), 3 Avenue de la Boétie, Pessac, France

\*fournier.j@icmcb-bordeaux.cnrs.fr

**Abstract:** Using luminescence confocal microscopy under 325 nm laser excitation, we explore the populations of defects existing in or at the vicinity of macroscopic surface flaws in fused silica. We report our luminescence results on two types of surface flaws: laser damage and indentation on fused silica polished surfaces. Luminescence cartographies are made to show the spatial distribution of each kind of defect. Three bands, centered at 1.89 eV, 2.75 eV and 2.25 eV are evidenced on laser damage and indentations. The band centered at 2.25 eV was not previously reported in photo luminescence experiments on indentations and pristine silica, for excitation wavelengths of 325 nm or larger. The luminescent objects, expected to be trapped in sub-surface micro-cracks, are possibly involved in the first step of the laser damage mechanism when fused silica is enlightened at 351 nm laser in nanosecond regime.

©2010 Optical Society of America

OCIS codes: (140.3330) laser damage; (180.2520) fluorescence microscopy.

---

## References and links

1. M. L. André, "Status of the LMJ project", in Solid state lasers for application to Inertial Confinement Fusion: Second Annual International Conference, M. L. André, ed., Proc. SPIE **3047**, 38–42 (1996).
2. E. M. Campbell, "The National-Ignition-Facility project," Fusion Technol. **26**, 755–766 (1994).
3. L. D. Merkle, N. Koumvakalis, and M. Bass, "Laser induced bulk damaged in SiO<sub>2</sub> at 1.064, 0.532 and 0.355 μm," J. Appl. Phys. **55**(3), 772–775 (1984).
4. J. Y. Natoli, B. Bertussi, L. Gallais, M. Commandré, and C. Amra, "Multiple pulses laser irradiation study in silica: comparison between 1064 and 355 nm", in *Advances in Optical Thin Films*, Claude Amra, Norbert Kaiser, H. Angus Macleod, Eds, Proceedings of SPIE **5250** 182–187 (2004)
5. L. Skuja, "Optically active oxygen-deficiency-related centers in amorphous silicon dioxide," J. Non-Cryst. Solids **239**(1-3), 16–48 (1998).
6. N. Bloembergen, "Role of cracks, pores, and absorbing inclusions on laser induced damage threshold at surfaces of transparent dielectrics," Appl. Opt. **12**(4), 661–664 (1973).
7. H. Bercegol, P. Grua, D. Hébert, and J. P. Morreeuw, "Progress in the understanding of fracture related damage of fused silica," in *Proceedings of Laser-Induced Damage in Optical Materials: 2007*, Gregory J. Exarhos, Arthur H. Guenther, Keith L. Lewis, Detlev Ristau, M. J. Soileau, Christopher J. Stolz, Eds, Proc. SPIE **6720**, 1–12 (2007)
8. S. G. Demos, M. Staggs, K. Minoshima, and J. Fujimoto, "Characterization of laser induced damage sites in optical components," Opt. Express **10**(25), 1444–1450 (2002).
9. M. R. Kozlowski, C. L. Battersby, and S. G. Demos, "Luminescence investigation of SiO<sub>2</sub> surfaces damaged by 0.35 mm laser illumination", in *Proceedings of Laser-Induced Damage in Optical Materials: 1999*, Gregory J. Exarhos, Arthur H. Guenther, M. R. Kozlowski, Keith L. Lewis, M. J. Soileau, Eds, Proc. SPIE **3902**, 138–144 (2000)
10. T. A. Laurence, J. D. Bude, N. Shen, T. Feldman, P. E. Miller, W. A. Steele, and T. Suratwala, "Metallic-like photoluminescence and absorption in fused silica surface flaws," Appl. Phys. Lett. **94**(15), 151114 (2009).
11. M. Kalceff, "Cathodoluminescence microcharacterization of the defect structure of irradiated hydrated anhydrous fused silicon dioxide," Phys. Rev. B **57**(10), 5674–5683 (1998).
12. A. N. Trukhin, and K. M. Golant, "Absorption and luminescence in amorphous silica synthesized by low-pressure plasmachemical technology," J. Non-Cryst. **353**(5-7), 530–536 (2007).

13. J. Néauport, P. Cormont, L. Lamainière, C. Ambard, F. Pilon, and H. Bercegol, "Concerning the impact of polishing induced contamination of fused silica optics on laser induced damage density at 351 nm," *Opt. Commun.* **281**(14), 3802–3805 (2008).
14. A. Anedda, C. M. Carbonaro, F. Clemente, and R. Corpino, "Ultraviolet excitation fine tuning of luminescence bands of oxygen deficient center in silica," *J. Appl. Phys.* **92**(6), 3034–3038 (2002).
15. J. Néauport, P. Cormont, P. Legros, C. Ambard, and J. Destribats, "Imaging subsurface damage of grinded fused silica optics by confocal fluorescence microscopy," *Opt. Express* **17**(5), 3543–3554 (2009).
16. H. Nishikawa, E. Watanabe, D. Ito, Y. Sakurai, K. Nagasawa, and Y. Ohki, "Visible photoluminescence from Si clusters in  $\gamma$ -irradiated amorphous SiO<sub>2</sub>," *J. Appl. Phys.* **80**(6), 3513–3517 (1996).
17. L. Skuja, "The origin of the intrinsic 1.9 eV luminescence band in glassy SiO<sub>2</sub>," *J. Non-Cryst.* **179**, 51–69 (1994).
18. Y. D. Glinka, S. H. Lin, L. P. Hwang, Y. T. Chen, and N. H. Tolk, "Size effect in self-trapped exciton photoluminescence from SiO<sub>2</sub>-based nanoscale materials," *Phys. Rev. B* **64**(8), 085421 (2001).
19. A. N. Trukhin, M. Goldberg, J. Jansons, H.-J. Fitting, and I. A. Tale, "Silicon dioxide thin film luminescence in comparison with bulk silica," *J. Non-Cryst.* **223**(1-2), 114–122 (1998).

## 1. Introduction

Fused silica damage at the wavelength of 351 nm (3.53 eV) in nanosecond regime is a major issue for the optimal operation of high power laser facilities, such as LMJ [1] or NIF [2] devices, devoted to inertial confinement fusion studies. Hence, lots of efforts are made in order to understand the involved damage mechanisms. While the intrinsic bulk damage threshold of high purity fused silica corresponds to fluences of about 100 J/cm<sup>2</sup> for 3 ns pulses [3], the surface damage one is in the 10 J/cm<sup>2</sup> range [4]. Such a difference of behavior is supposed to be induced by defects existing in fused silica subsurface. From a structural point of view, two luminescent defects are well known in silica [5]: the ODC (Oxygen Deficient Center) and the NBOHC (Non Bridging Oxygen Hole Center). But these defects are known to exhibit a very low absorption at 351 nm (3.53 eV) and would produce low yield emission as long as the excitation wavelength is above the absorption spectral range. From a macroscopic point of view, surface and subsurface fractures are recognized for a long time to be possible damage precursors [6]. Recent attempts have been made to model interaction between subsurface cracks and laser [7]. Hence, in order to identify a defect that could trigger damage at 351 nm (3.53 eV), many works have been focused on pristine polished fused silica surfaces as well as on surface flaws (indentation and laser damage). Demos and Kozłowski studied laser damage sites using photoluminescence spectroscopy [8,9]. They reported the existence of two or three luminescence bands depending on the damage site considered. Two major bands are observed, peaking at 560 nm (2.21 eV) and 650 nm (1.90 eV). The first one is not attributed to a known defect, while the second band is attributed to the NBOHC defect [5]. A third band centered at 450 nm (2.75 eV), which is due to ODC's [5], is significantly observed only in laser damage sites. Laurence et al. [10] performed high sensitivity time resolved photoluminescence confocal microscopy on laser damage sites and indentations, however luminescence spectra were not shown in this paper. They reported a fast photoluminescence signal linked to strongly absorbent areas in laser damage. Using cathodoluminescence micro characterization, Kalceff has studied anhydrous and hydrated amorphous silicon dioxide [11], showing the presence of four luminescence bands around 1.9 eV (650 nm), 2.40 eV (516 nm), 2.75 eV (450 nm), and 3.1 eV (401 nm) at room temperature. At low temperature (5 K), the same peaks are present but the ratio of the different contributions is changed. Trukhin, besides the ODC contributions saw also the unattributed 560 nm (2.21 eV) luminescence band on amorphous silica synthesized by low-pressure plasma chemical technology [12]. We then conclude that if ODC and NBOHC defects are regularly seen, the 560 nm band is randomly reported and unexplained.

In this paper, we investigate defects using luminescence confocal microscopy. This technique offers the advantage of making high resolution spatial mapping of surfaces, providing the luminescence spectrum of each measurement point. This technique is used on different samples: laser damage sites and indentations realized on polished fused silica samples, as well as loose abrasive lapped samples. The goal of this work is to obtain luminescence surface mappings and spectra at the same time on each sample.

In Section 2, the sample preparation methods are detailed; then we describe the equipment used for luminescence confocal microscopy and the calibration method used to correct the spectra from the equipment. Section 3 is devoted to the luminescence mappings that we obtained, the results are discussed in Sec.4, and conclusions are drawn in Sec.5.

## 2. Experimental arrangement

### 2.1 Sample preparation methods

Experiments were conducted on 50 mm diameter; 5 mm thick high purity super polished fused silica samples. Samples were polished with a process ensuring a low cerium content in the fused silica interface [13]. Before measurements, all the samples were thoroughly cleaned in order to prevent any external pollution on studied surfaces and surface flaws, which could interact with the excitation radiation. The sample cleaning was made using a basic soap based bath followed by an acid bath solution in ultrasonic baths under laminar flux. Drying of samples was performed by lift-off technique, i.e. slowly lifting the sample from the last bath to avoid any drying traces on the surfaces. Then, they were stored in sealed cleaned boxes. Before each measurement, an additional drag-wipe of the surface was performed using ultrapure ethanol.

Indentations were made with a spheroconical diamond tip of 20  $\mu\text{m}$  diameter (Nanoindenter NanoTest NT-600, manufactured by Micro Materials Ltd, Wrexham, Great Britain). The applied load is 1.5 N, the loading rate (until the final load) is 2000 mN/s, and the maximum load is maintained during 60 s.

Laser damage was created using a Nd:YAG laser, at a 351 nm (3.53 eV) wavelength with pulse duration of 2.5 ns, and a 6 mm beam diameter. For each damage site, we used a multi-shot technique (one to seven shots per site) in order to obtain different sizes of damage.

### 2.2 Photo-luminescence confocal microscopy

Photoluminescence spectra were carried out on a LABRAM HR-800 spectrometer, a high resolution Raman spectrometer with luminescence confocal microscopy capabilities (Fig. 1).

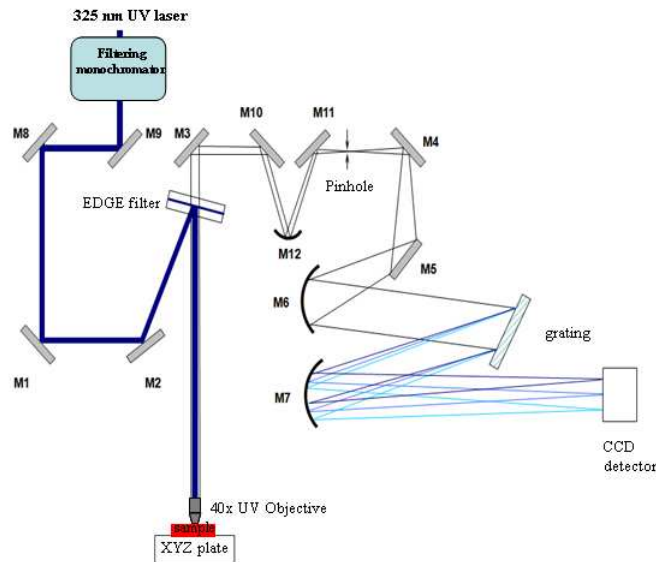


Fig. 1. General scheme of photo-luminescence spectrometer. M1 to M12 a mirrors used to convey the laser beam and luminescence signal. The EDGE filter is used to reject the 325 nm excitation from the luminescence signal. The grating and CCD detector defines the spectrometer resolution.

Luminescence is excited by a 325 nm (3.81 eV) continuous He/Cd laser at room temperature. The focal spot size on the sample is about  $1 \mu\text{m}^2$  and the maximal power is 10 mW. The excitation source is separated from the emission using an EDGE filter. The pinhole is used for collecting only the luminescence coming from the analysed focal plan and the signal is collected with a CCD camera. The spatial resolution of this spectrometer is about 1  $\mu\text{m}$ . The pinhole is opened at 300  $\mu\text{m}$  because of the weakness of the luminescence emitted by the samples. For our reference sample (a silica sample without artificial surface defect), we used a 100  $\mu\text{W}$  laser power since signal was rather weak. For the other samples, a 10  $\mu\text{W}$  laser power was retained. This choice of low power was made after photobleaching measurements in order to ensure that photobleaching was negligible at this power. This was compensated by using a long time signal accumulation in order to keep a good spectral resolution (1 nm) which is a key point for our analysis. All the intensities are expressed in cps (number of counts per second on the CCD). We also outline that an offset of some cps can occur; this signal being due to the electronic noise.

For all measurements, the obtained spectra were corrected for the spectral response of the spectrometer. The calibration was made using a tungsten lamp, the spectrum of which is provided by the supplier. In order to avoid detector saturation, the pinhole was closed at the maximum (5  $\mu\text{m}$ ) and a filter was used to reduce the lamp flux. The same filter was used to reduce the laser flux in all our experiments. The obtained response of the spectrometer is shown in Fig. 2.

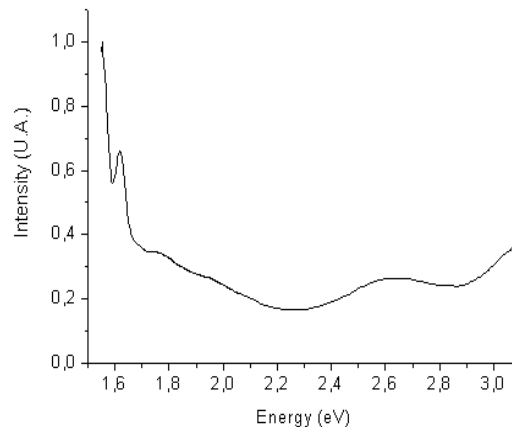


Fig. 2. Response of the spectrometer used to correct photo-luminescence spectra.

### 3. Results

#### 3.1 High purity silica

We conducted our first experiments on pristine, cleaned polished fused silica samples. A typical measured spectrum is depicted in Fig. 3.

Under excitation at 3.81 eV (325 nm), the pristine silica yields a luminescence band around 2.75 eV (450 nm). The experimental signal was fitted with a multiparameter Gaussian function. This analysis reveals the existence of two luminescence bands centered at 2.25 eV (551 nm) and 2.75 eV (450 nm). The parameters of the fit are given in Table 1.

Luminescence cartographies were made at the surface of pristine silica. Scanning is done with a 3  $\mu\text{m}$  step, the size of the analyzed area is 20  $\mu\text{m} \times 20 \mu\text{m}$ . We have observed that the distribution of the defects is homogeneous and that the defect at 450 nm (2.75 eV) prevails.

The band at 2.75 eV is known to be induced by ODC defects [5,9,11]. We measure a FWHM of 0.75 eV for this peak. This width is still the object of some disagreements. If Skuja reports a 0.34 eV FWHM for a 3.15 eV excitation [5], Anedda measures a FWHM of about 1eV on commercial silica samples [14]. We see that ODC is the main defect existing on

polished silica surfaces. The 2.25 eV band that we weakly see was already seen before [11,12,15,16] but its interpretation is still the object of controversy.

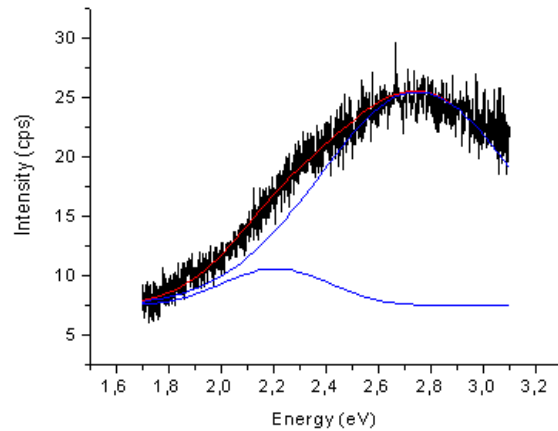


Fig. 3. Photo-luminescence spectrum of pristine silica under 3.81 eV excitation. Experimental signal (black), fitted signal (red) Gaussian components of the fitted luminescence signal (blue).

**Table 1. Fit parameters obtained for luminescence spectra of pristine silica: mean emission energies and mean FWHM (Full Width at Half Maximum) of the resolved Gaussian components.**

|          | Position (eV) | FWHM (eV) |
|----------|---------------|-----------|
| 1st Band | 2.75          | 0.75      |
| 2nd Band | 2.25          | 0.4       |

### 3.2 Indentation

We then focused on surface flaws and first considered indentations. Figure 4 shows a transmission microscopy image of such an indentation. Different sites are investigated. Site A and C are located on the periphery of the scanned area, out of the indent. Site B is located in the central region of the indent, as shown in Fig. 4. The corresponding spectra obtained respectively on site A and B are shown in Fig. 5. The spectrum obtained for site C is not given. Though significant signal ( $I_{\max} = 30$  cps) is obtained in site A, the signal in site C is at the noise level ( $I_{\max} < 5$  cps).

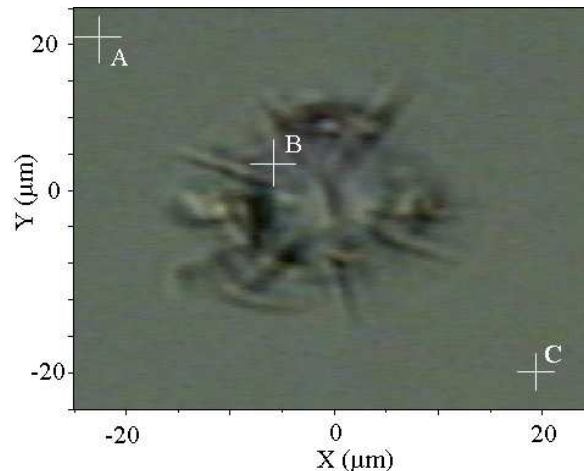


Fig. 4. Image in transmission microscopy of an indent; the three sites (A, B and C) are the points under investigation.

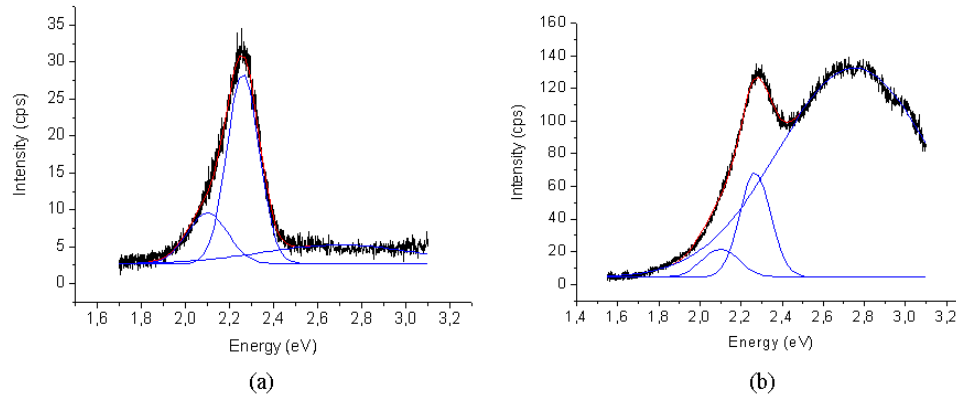


Fig. 5. Photo-luminescence spectra for indents, excitation at 3.81 eV (325 nm). (a) Site A. (b) Site B. Experimental signal (black), fitted signal (red) Gaussian components of the fitted luminescence signal (blue)

As previously, experimental signals were analyzed with a multiparameter Gaussian function. Obtained parameters are summarized in Table 2. In site A, i.e. far from the indent imprint, and in site B, i.e. in the indentation, the spectrum is composed of three luminescence bands: the first one is centered at 2.1 eV (590 nm), the second one at 2.25 eV (551 nm) and the third at 2.75 eV (450 nm). This last spectral band is very weak in site A.

We can observe a significant increase (of a factor close to 10 for site B and close to 3 for site A) in the band intensities at 2.25 eV and 2.75 eV when compared to pristine silica.

**Table 2. Parameters used for fitting the two obtained spectra on site A and site B of an indent.: mean emission energies and mean FWHM of the resolved Gaussian components.**

|          | Position (eV) | FWHM (eV)    |
|----------|---------------|--------------|
| 1st band | Site A: 2.75  | Site A: 0.7  |
|          | Site B: 2.75  | Site B: 0.73 |
| 2nd band | Site A: 2.25  | Site A: 0.14 |
|          | Site B: 2.25  | Site B: 0.15 |
| 3rd band | Site A: 2.10  | Site A: 0.14 |
|          | Site B: 2.10  | Site B: 0.17 |

To get knowledge of the spatial distribution of defects, we made luminescence spectroscopy images of the indentation on an area of 45  $\mu\text{m}$  x 45  $\mu\text{m}$  with a scanning step of 2  $\mu\text{m}$ . We can see in Fig. 6 the evolution of the defect locations. The 2.25 eV defect seems to be the major one in both indent and surrounding areas. Most of the defects are concentrated on the edges of the indent. As can be observed in Fig. 6, the luminescence signal is at the noise level all around the indent except in the region of site A. This observation invalidates the attribution of this band to pollutants, as for example organic contamination or ceria doping resulting from final stage of polishing, since in such cases the green luminescence should appear randomly distributed on the sample surface and not only in fractures. Hence, the luminescence spectra are clearly the signature of silica defects in surface and subsurface cracks formed during the creation of the indent.

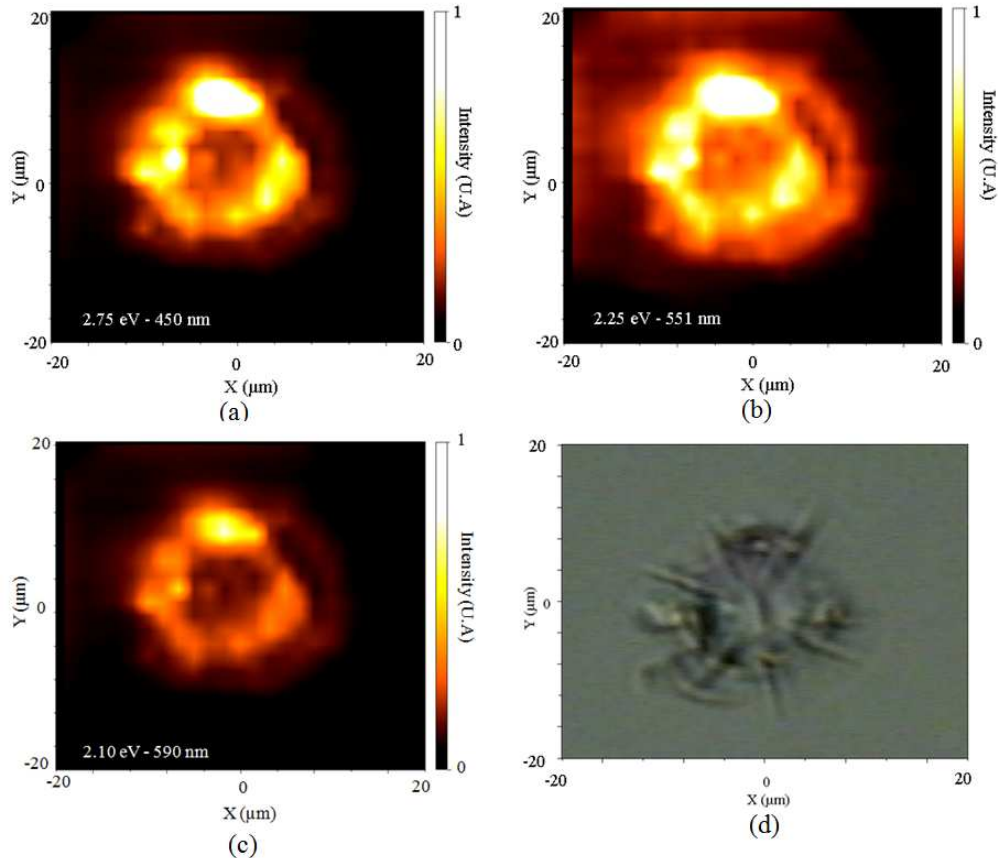


Fig. 6. Photo-luminescence cartographies obtained on indentation under 3.81 eV excitation. (a): cartography for 2.75 eV emission. (b): cartography for 2.21 eV emission. (c): cartography for 2.10 eV emission. (d): image in transmission microscopy of laser damage.

In the two cases, the three same luminescence bands are present. One of them is well known and it is the 2.75 eV band which is attributed to ODC defect [5]. The band at 2.25 eV, as previously said, has already seen but not interpreted yet. Finally the band at 2.1 eV can be NBOHC.

### 5.3 Laser damage

Figure 7 shows an image in transmission microscopy of the analyzed laser damage. Three sites denoted respectively A, B and C are presented. Site A is situated inside the strongly crackled area of the laser damage, while site B is in a less crackled area. Site C is located on the edge of the laser damage. The photo-luminescence spectra of each site are shown in Fig. 8.

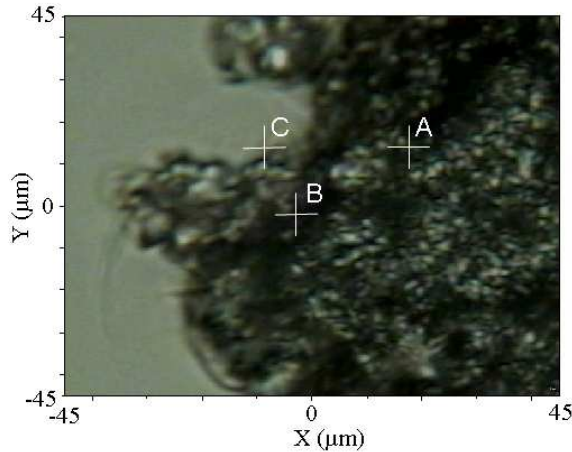


Fig. 7. Image in transmission microscopy of front-surface laser damage. The three points A, B and C are the studied sites.

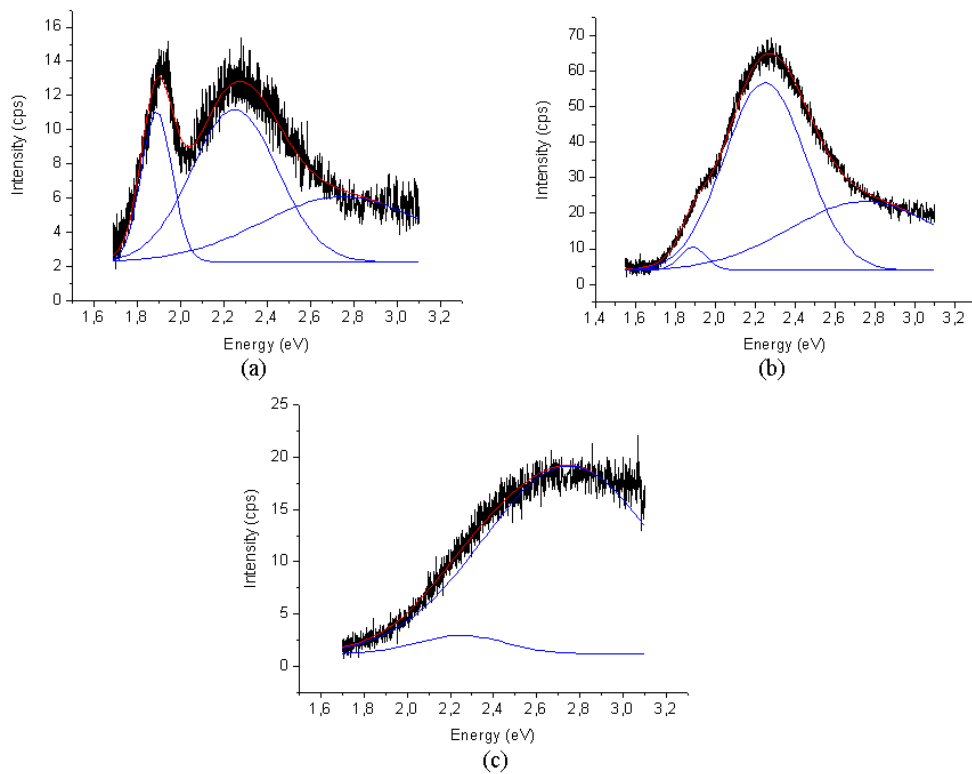


Fig. 8. Photo-luminescence spectra for laser damage, excitation at 3.81 eV (325 nm). (a) Site A. (b) Site B. (c) Site C. Experimental signal (black), fitted signal (red) Gaussian components of the fitted luminescence signal (blue).

As previously, experimental signals were analyzed with a multiparameter Gaussian function. Obtained parameters are summarized in Table 3. In site A i.e. inside the strongly crackled area of the laser damage, and in site B, i.e. in the less crackled area, the spectrum is composed of three luminescence bands: the first one is centered at 1.89 eV (656 nm), the second one at 2.25 eV (551 nm) and the third at 2.75 eV (450 nm). Finally, the spectrum

obtained in site C, i.e. at the edge of the laser damage is composed of two bands at 2.25 eV (551 nm) and 2.75 eV (450 nm) as in pristine silica.

Regarding intensities comparison with pristine silica and indentation is not possible since the analysed volume changed inside the damage crater.

**Table 3. Parameters used for fitting the three spectra obtained for laser damage: mean emission energies and mean FWHM of the resolved Gaussian components.**

| Laser Damage | Position (eV) | FWHM (eV)    |
|--------------|---------------|--------------|
| 1st band     | Site A: 2.75  | Site A: 0.75 |
|              | Site B: 2.75  | Site B: 0.75 |
|              | Site C: 2.75  | Site C: 0.75 |
| 2nd band     | Site A: 2.25  | Site A: 0.39 |
|              | Site B: 2.25  | Site B: 0.40 |
|              | Site C: 2.25  | Site C: 0.40 |
| 3rd band     | Site A: 1.89  | Site A: 0.14 |
|              | Site B: 1.89  | Site B: 0.13 |
|              | Site C: none  | Site C: none |

Figure 9 shows luminescence cartographies where the analysed area is of  $90 \mu\text{m} \times 90 \mu\text{m}$  with a scanning step of  $4 \mu\text{m}$ . The defect at 1.89 eV is located in the laser damage contrary to the defects at 2.25 eV and 2.75 eV which are located in and out of the damage, particularly the defect at 2.75 eV which is present far from the edge of the damage.

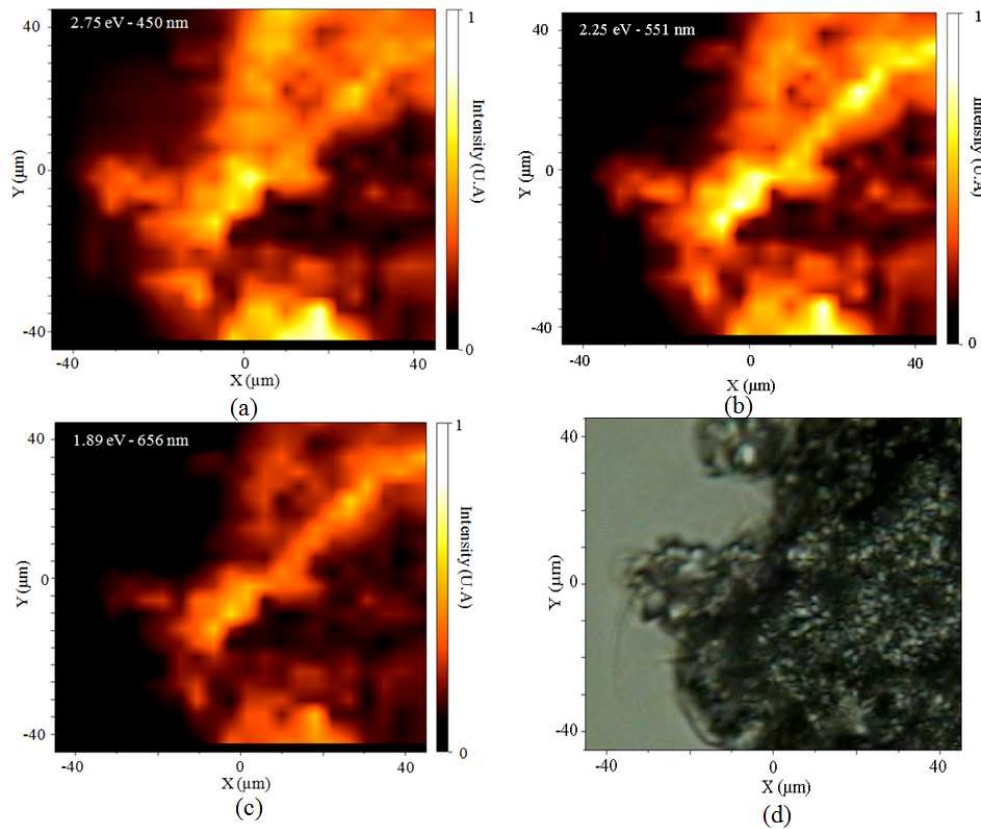


Fig. 9. Photo-luminescence cartographies obtained on laser damage, under 3.81 eV excitation. (a): cartography for 2.75 eV emission. (b): cartography for 2.21 eV emission (c): cartography for 1.89 eV emission (d): image in transmission microscopy of laser damage.

In laser damage, three luminescence bands have been detected at 1.89 eV, 2.25 eV and 2.75 eV. At the edge of the laser damage, two luminescent bands at 2.25 eV and 2.75 eV have been observed. The bands at 1.89 eV and at 2.75 eV are well known and are attributed to

NBOHC defect for the first one and to ODC defect for the second [5]. The band at 2.25 eV is found again in site A, B and C.

#### 4. Discussion

All the spectra on the studied surface flaws show the presence of at least two or three luminescence bands. If two of them have been previously studied in detail and attributed to specific defects in glass silica (1.89 eV: NBOHC and 2.75 eV: ODC), the band at 2.25 eV found in indentation, laser damage, and probably to a very less extent on pristine silica is not clearly interpreted though already observed in laser damage [8,9]. Even if the 2.75 eV band is unambiguously attributed to ODC [5,8,9], it must be noticed that under 3.81 eV excitation, only low yield luminescence should be observed. Concerning the NBOHC, its absorption remains very weak under 3.81 eV excitation. It is interesting to comment its position at 2.1 eV in indentation. It could be attributed to the luminescence signal of surface NBOHC. According to Skuja, a two-component luminescence band of crushed silica in an inert atmosphere is peaking at 1.93 eV and 1.98 eV while bulk luminescence is observed at 1.93 eV [17]. The largest energy component is then characteristic of surface centers and can be compared to our observation in indentation. Furthermore, Glinka has shown that, in different type of silica (mesoporous, nanoparticles...), the luminescence bands of Self Trapped Exciton (STE) and NBOHC may appear at different energy position [18].

A band at 2.25 eV has already been characterized (position and width) in defect structure initiated by cathodoluminescence (resp.  $\gamma$ -irradiation) in hydrated and anhydrous silica glasses (resp. amorphous silica). It has been attributed to STE (resp. E'-type defects formed in SiO<sub>x</sub> environment) [11,16]. Involvement of STE luminescence should not be observed for ambient temperature, nevertheless Trukhin showed that, at room temperature, the luminescence signal is not equal to zero [12]. In another contribution on silicon dioxide thin film luminescence, the same author linked this signal to a network luminescence [19]. Our main interesting result is the observation of relatively intense peak with narrow width in and around indentations. It can be suggested that it is due to mechanical stress trapped in cracks inducing contraction of the silica network. Local structure characterizations have to be performed to clarify this point. However, the STE luminescence requires electron transitions from silica valence band towards conduction band through multistep absorption. This process could be allowed by the presence of a high density of states in the forbidden gap.

#### 5. Conclusion

In this work, we have shown photo-luminescence spectra and cartographies obtained on pristine silica, indentation and laser damage. On pristine silica, two luminescence bands at 2.25 eV (551 nm) and 2.75 eV (450 nm) have been observed. For indentation and laser damage, three luminescence bands at 2.1 eV (590 nm) in indentation and 1.89 eV (656 nm) in laser damage, 2.25 eV (561 nm) and 2.75 eV (450 nm) have been emphasized. The bands at 1.89 eV and 2.75 eV are attributed to NBOHC and ODC defect respectively. The 2.25 eV band, yielding to a very strong intensity in indentation, is not still clearly ascribed. Photo-luminescence cartographies on indentation show that NBOHC and ODC defects are found inside the indent, while the 2.25 eV luminescence appears in the indent and in its surrounding. In the contrary for laser damage, the NBOHC defect is only located inside the damage, while ODC defect is spread over a large area. Some potential mechanisms explained the presence of the 2.25 eV and its evolution in width are proposed ; they shall be verified during further experiments.

#### Acknowledgments

We thank H. Bercegol for active contribution to these results, T. Cardinal and A. Garcia for fruitful discussions concerning luminescence spectroscopy, and T. Donval for assistance with laser damage accomplishment.